Electronic Supplementary Material (ESI) for EES Catalysis.

– Electronic Supplementary Information –

Local hydrophobicity allows high-performance electrochemical carbon monoxide reduction to C2+ products

Attila Kormányos,[a] Balázs Endrődi[a,]*, Zheng Zhang[a], Angelika Samu[a], László Mérai[a], Gergely F. Samu[a,b], László Janovák[a], and Csaba Janáky[a,b,]**

[a]University of Szeged, Department of Physical Chemistry and Materials Science, Aradi sq. 1, Szeged, 6720, Hungary

[b]ELI-ALPS, ELI-HU Non-Profit Ltd., Wolfgang Sandner 3, Szeged H-6728, Hungary

*Correspondence: endrodib@chem.u-szeged.hu

**Correspondence: janaky@chem.u-szeged.hu

Morphology of the Capstone ST-110 containing catalyst layers

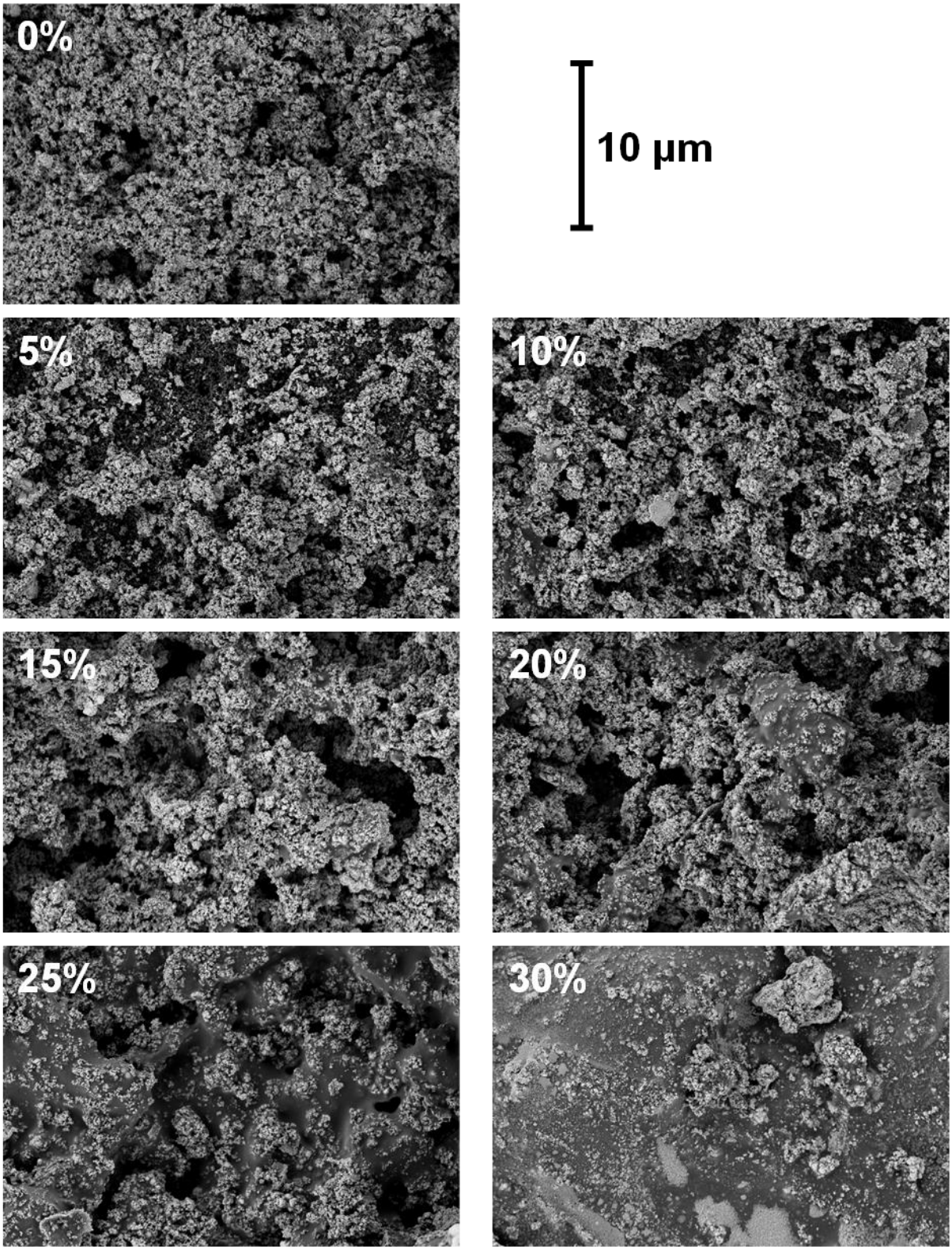

Figure S1. SEM images recorded for the Cu NP GDEs with different CST content (wt%, as indicated in the images).

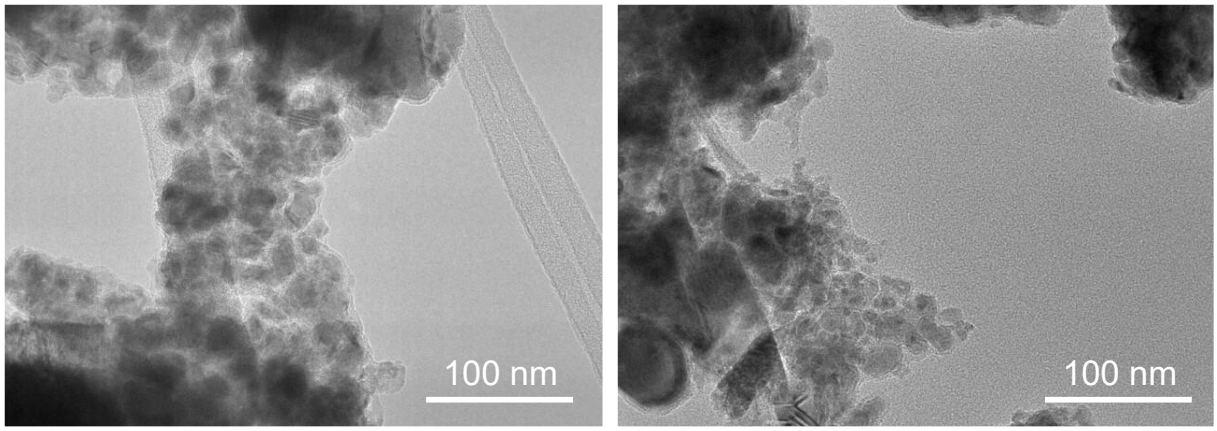

Figure S2. TEM images captured from the bare Cu NPs and that were used for the calculation of the particle size distribution.

Structure and gas adsorption properties of the Capstone ST-110 binder

The structure of the Capstone ST-110 (CST) pore sealer polymer is a trade secret that is not shared with the end users However, based on the safety data sheet of the material ,it is a "terpolymer of fluorinated alkyl-methacrylates, dialkylammoniumalkyl methacrylate acetate salts, and aliphatic acids". Based on former studies on the importance of nitrogen moieties in the catalysts layer in the case of electrochemical CO_2 reduction, we assume that any specific interaction of the polymer and the reactant gas (CO in our case) might be related to this part. In **Figure S3**, we, therefore, show the general structure of the N-containing block of the polymer. Interestingly, a pendant quaternary ammonium group is attached to the polymer backbone. We mention that this motif is very similar to what is seen in generally applied anion exchange membranes and ionomers.

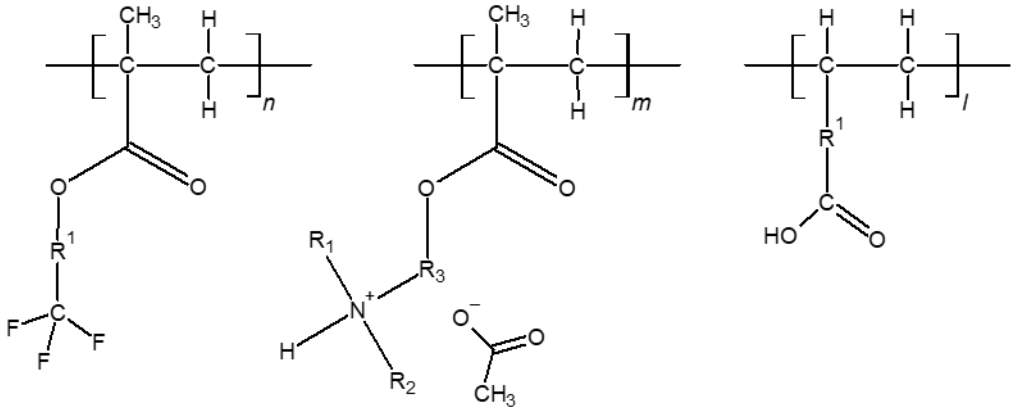

Figure S3. The assumed general structure of the 3 monomers of the Capstone ST-110 terpolymer, as derived from the safety data sheet of the material. Note that the exact formula is a trade secret and therefore it is not disclosed with the end-users.

The gas adsorption properties of the Capstone ST-110 polymer were evaluated in quartz crystal microbalance (QCM) measurements. A thin film of the polymer was formed on Au-coated quartz crystals by drop-casting (ca. 300 μg polymer). After drying, the polymer coated QCM crystal was placed in the resonator head, that was mounted in a sealed gas chamber. The gas chamber was purged with Ar, CO or CO_2 gas at a gas flow-rate of 50 $cm^3\ min^{-1}$. The mass change was calculated from the Sauerbrey equation ($\Delta f = -C \times \Delta m$), using a constant value of $C = 56.6\ \text{Hz}\ \mu g^{-1}\ cm^2$, as provided in the manual of the SRS QCM200 instrument. Based on the QCM measurements (**Figure S4**), no specific CO adsorption occurs on the Capstone ST-110 polymer. On the other hand, we could prove the adsorption of carbon dioxide,

suggesting that this binder might aid the reactant adsorption during the electrochemical reduction of CO_2 (CO2RR).

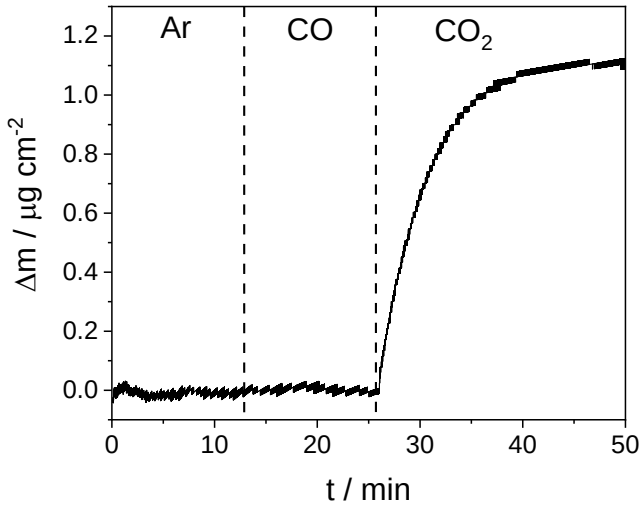

Figure S4. QCM measurements on Capstone ST-110 coated quartz crystals (Au coated), meanwhile purging the gas chamber around the sample with u = 50 cm^3 min^{-1} Ar, CO or CO_2 gas, as shown in the figure.

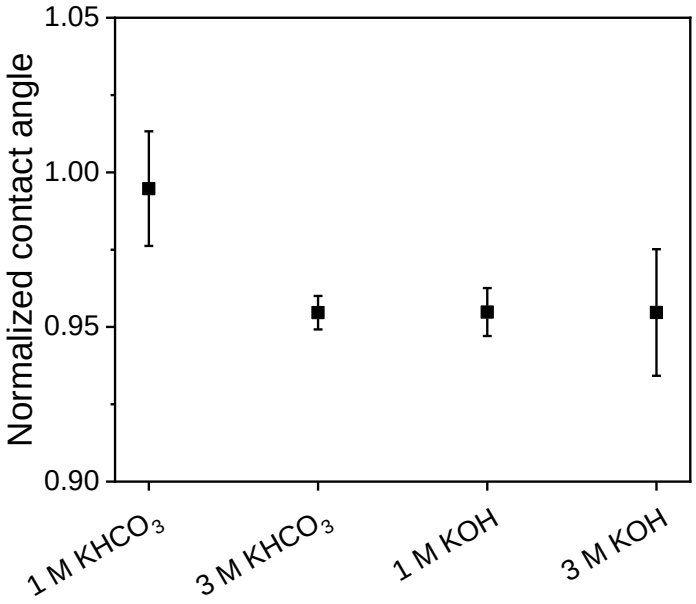

Figure S5. Normalized contact angles measured in various electrolytes at Cu NPs GDE with 5 wt% CST content. Contact angles were normalized by the average contact angle measured using pure water.

Microfluidic electrolyzer cell used for the electrochemical CO reduction (CORR) measurements

The CORR measurements were performed in a single electrolyte-separated microfluidic electrolyzer cell (**Figure S3**), with an active surface area of A = 1 cm^2.

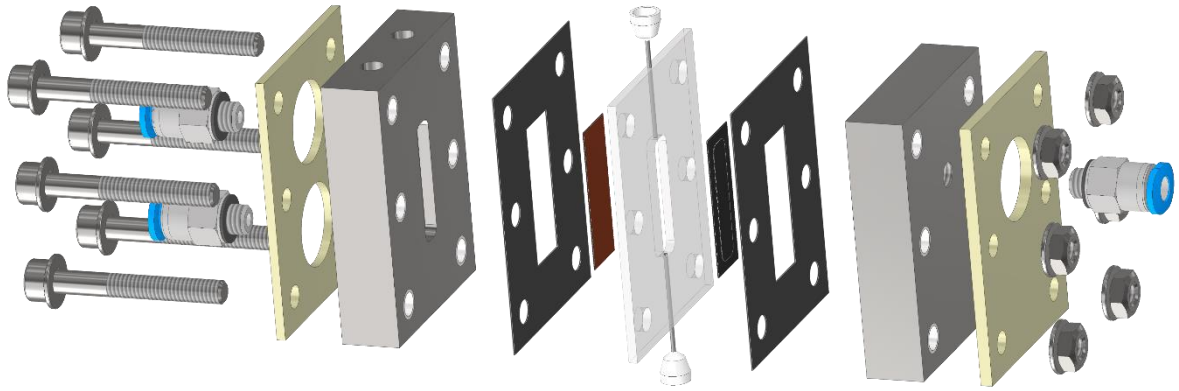

Figure S6. Schematic exploded view of the used microfluidic electrolyzer cell. The window size on the flow channel is 0.5 cm × 2 cm.

Electrochemical CO reduction measurements using Capstone ST-110 (CST) binder

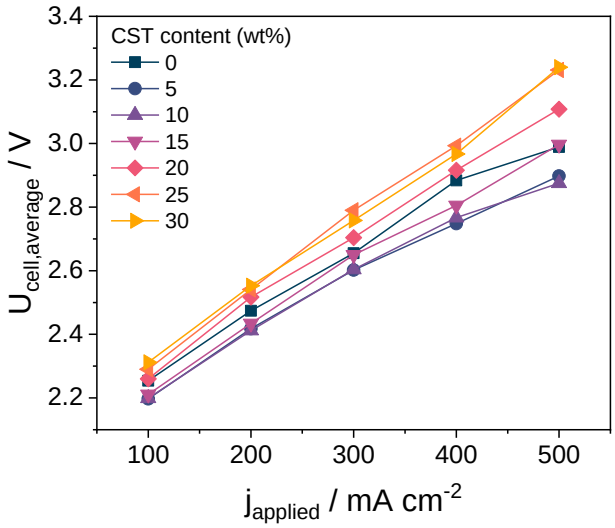

Figure S7. Averaged cell voltages measured during chronovoltammetric CORR measurements using samples with varying CST content at applied current densities between 100-500 mA cm^{-2}. The measurements were performed at room temperature, applying a single 1 M KOH electrolyte solution. The CO gas flow rate was 26.5 sccm, while the electrolyte solution was fed at a rate of 0.5 cm^3 min^{-1}. The lines among the data points serve only as a guide to the eyes.

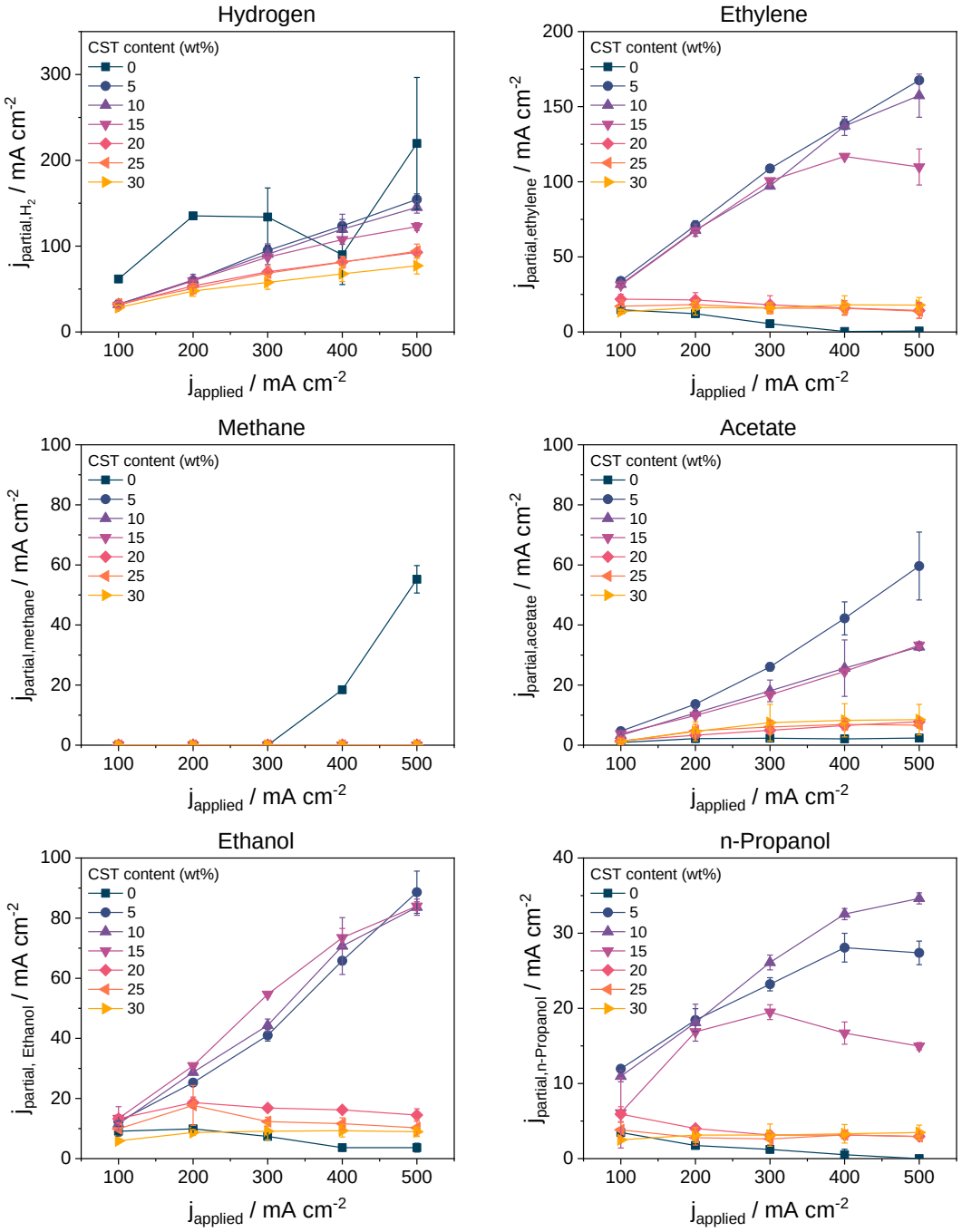

Figure S8. Product formation rates during CORR at different current densities, using catalyst layers containing 1 mg cm^{-2} d < 25 nm Cu nanoparticles and different amounts of CST binder. The measurements were performed at room temperature, applying a single 1 M KOH electrolyte solution. The CO gas flow rate was 26.5 sccm, while the electrolyte solution was fed at a rate of 0.5 cm^3 min^{-1}. The lines among the data points serve only as a guide to the eyes.

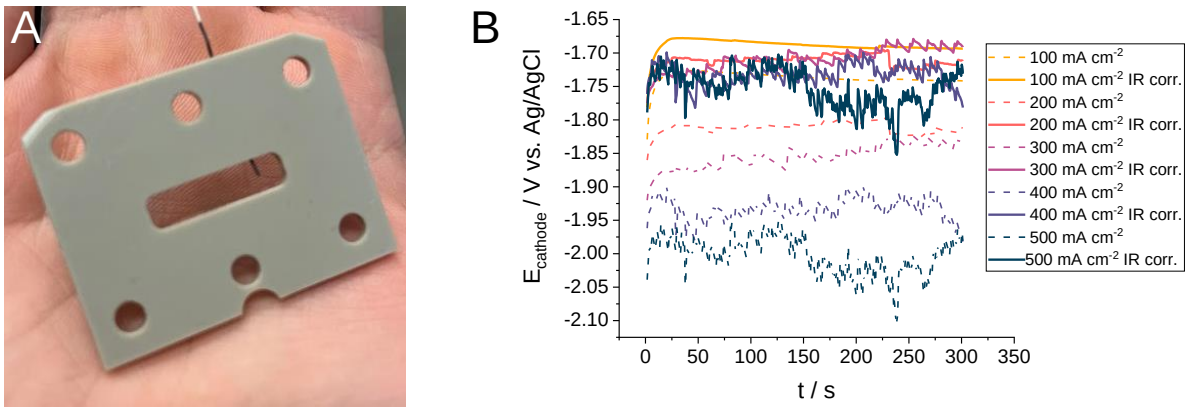

Fig. S9. (A) Photograph taken of the reference electrode in the microfluidic flow element. (B) Uncompensated and IR-corrected cathode potential recorded during chronovoltammetric experiments applying various current densities using a Cu NPs+5% CST sample and a 1 M KOH electrolyte solution. The electrolyte flow rate was 1 cm^3 min^{-1}, while the CO flow rate was fixed at 26.5 sccm. Solution resistance was determined by conducting current interruption measurements at each applied current density prior to the chronovoltammetric experiments. 85% of this value was used for the IR correction.

Current density / mA cm^{-2}	R_s / Ω
100	0.602
200	0.628
300	0.630
400	0.627
500	0.666

Table S1.: R_s values determined by performing a current interruption measurement prior to the chronopotentiometry experiment.

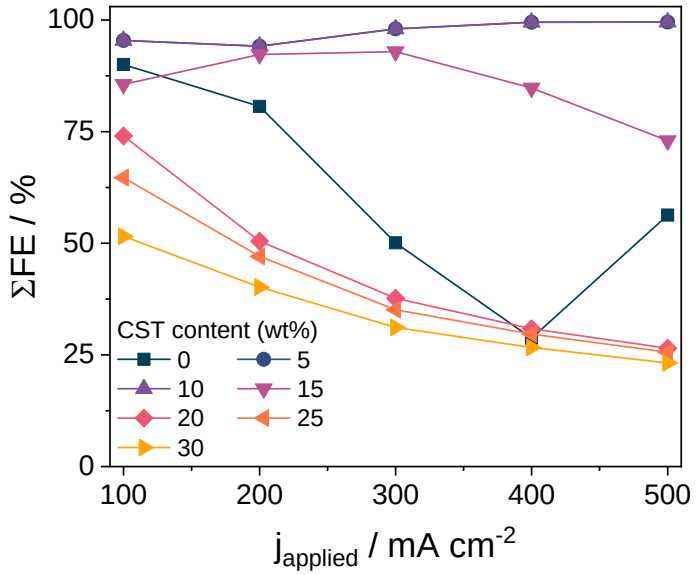

Figure S10. The total FE during the measurements presented in **Figure S5**. The total FE was calculated by summing up the partial current densities determined for the formation of different products, dividing it by the total current density, and multiplying it by 100% (to transform to the percentage scale). The lines among the data points serve only as a guide to the eyes.

At higher binder contents, the total FE remained notably below 100 %, in some cases, we could only account for 20-30% of the total charge. We assumed that the formation of gas products in the liquid stream (or their breakthrough) is behind this phenomenon. Therefore, we modified our experimental setup to collect the gas products from both the gas outlet port of the cell and from the electrolyte solution after liquid-gas separation (**Figure S8**). As detailed in the manuscript (**Figure 2D**), a large amount of hydrogen was detected that left the electrolyzer cell together with the liquid stream.

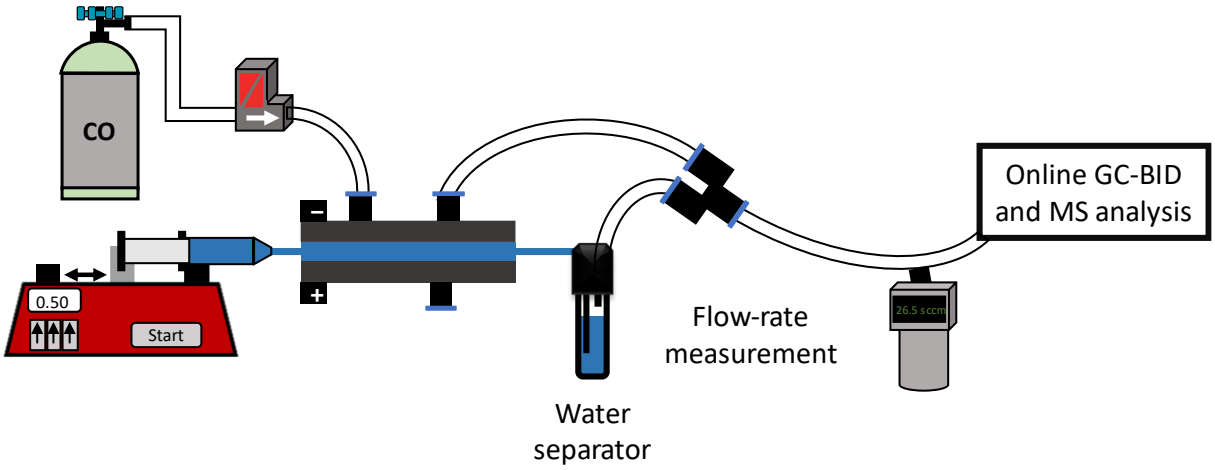

Figure S11. Schematic drawing of the experimental setup used for studying the gas products formed in the gas and liquid phases together.

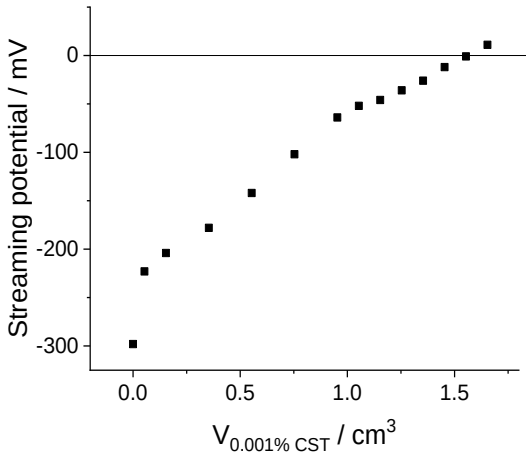

Fig. S12. Determination of the amount of the electrostatically adhered CST on the surface of CuNPs.

Electrochemical CO reduction measurements using Nafion binder and PTFE particles containing catalyst layers

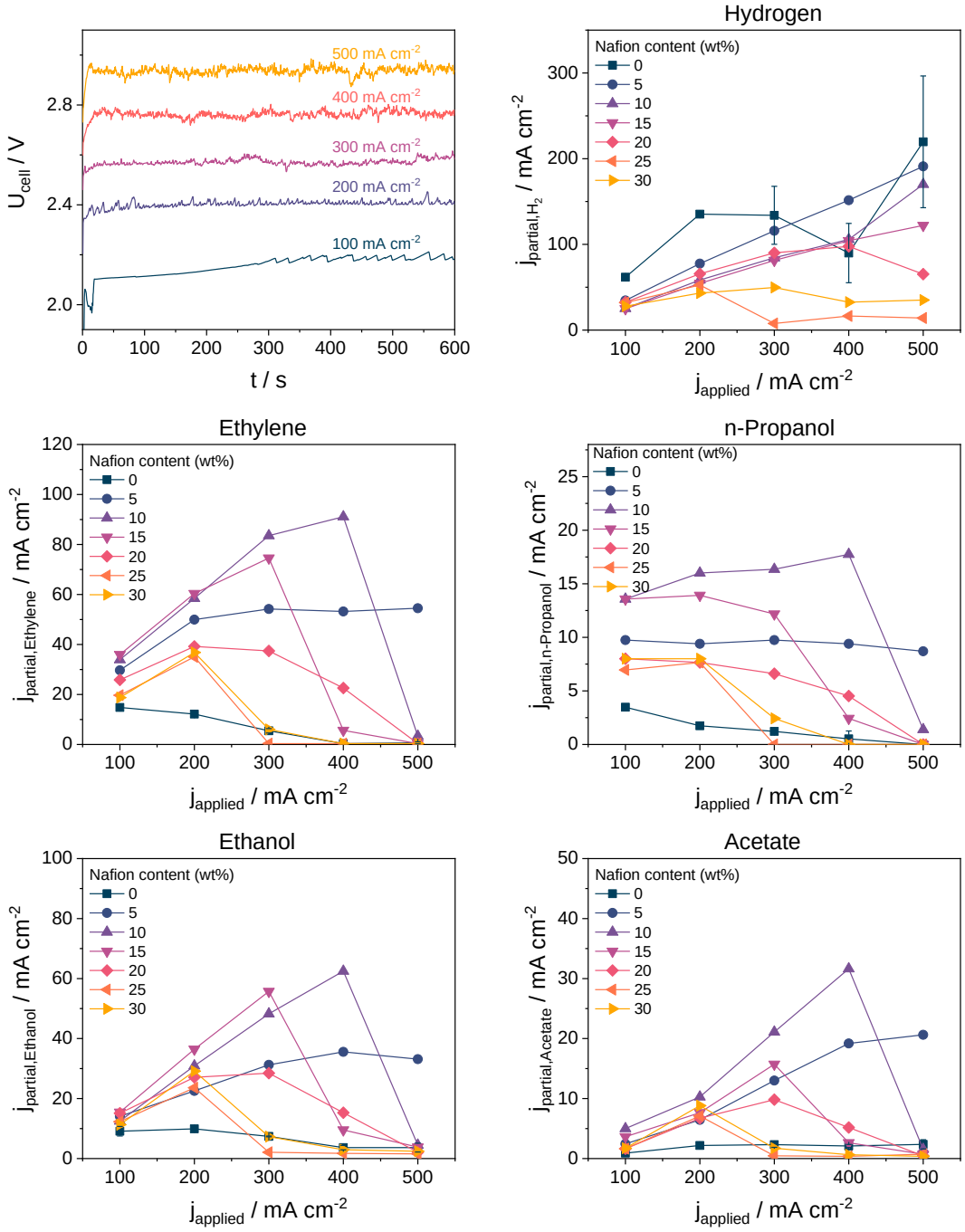

Figure S13. (A) Chronovoltammetry curves and product formation rates during CORR at different current densities, using catalyst layers containing 1 mg cm^{-2} d < 25 nm Cu nanoparticles and different amounts of Nafion binder. The measurements were performed at room temperature, applying a single 1 M KOH electrolyte solution. The CO gas flow rate was 26.5 sccm, while the electrolyte solution was fed at a rate of 0.5 cm^3 min^{-1}. The lines among the data points serve only asa guide to the eyes.

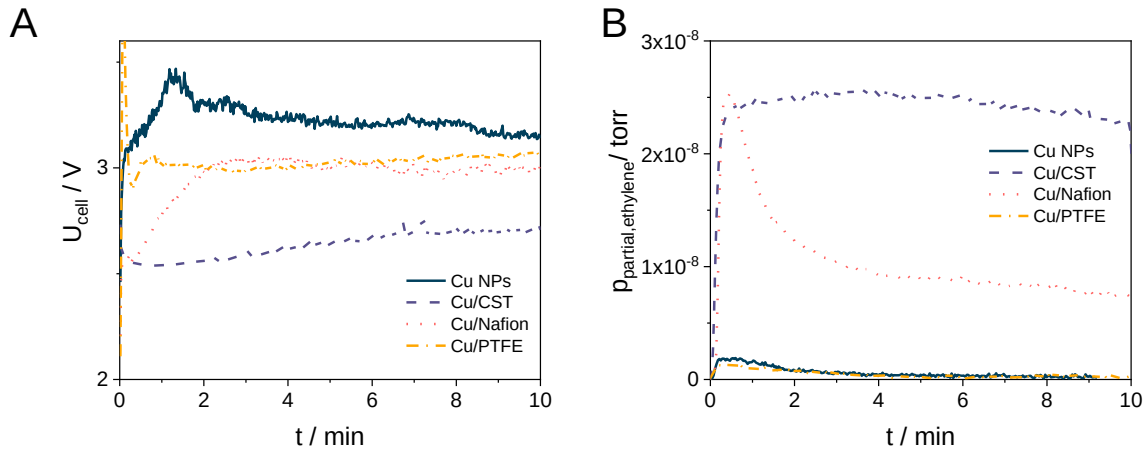

Figure S14. (A) Chronovoltammetry curves and (B) ethylene formation rate from mass spectrometry measurements during CORR at 500 mA cm^{-2} current density, using Cu NP GDEs with different binders. The amount of the binder was 5 wt% in all cases. The measurements were performed at room temperature, applying a single 1 M KOH electrolyte solution. The CO gas flow rate was 26.5 sccm, while the electrolyte solution was fed at a rate of 0.5 cm^3 min^{-1}.

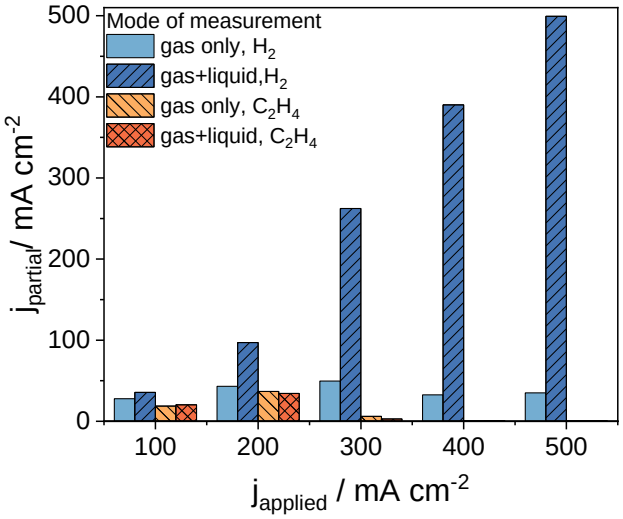

Figure S15. Product distribution obtained by performing electrolysis measurements at different current densities using 5 wt% Nafion and Cu NPs containing GDE cathodes. The amount of the formed gas products were either recorded only from the gas outlet stream ("gas only") or by connecting the gas and liquid outlet stream after a water separator unit ("gas+liquid").

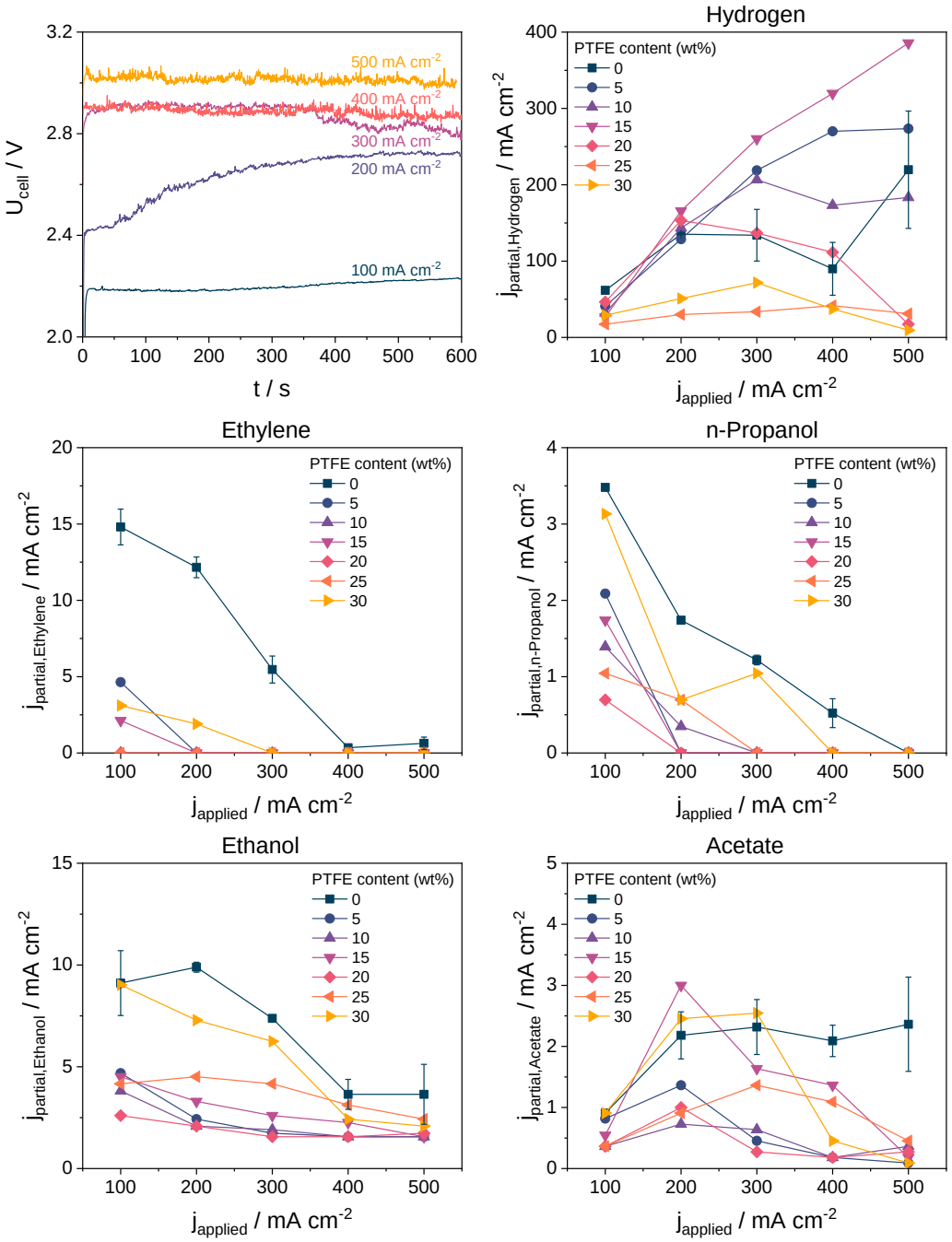

Figure S16. (A) Chronovoltammetry curves and product formation rates during CORR at different current densities, using catalyst layers containing 1 mg cm^{-2} d < 25 nm Cu nanoparticles and different amounts of PTFE particles as a binder. The measurements were performed at room temperature, applying a single 1 M KOH electrolyte solution. The CO gas flow rate was 26.5 sccm, while the electrolyte solution was fed at a rate of 0.5 cm^3 min^{-1}. The lines among the data points serve only as a guide to the eyes.

Topology of the CST containing Cu NP GDEs used in CORR experiments

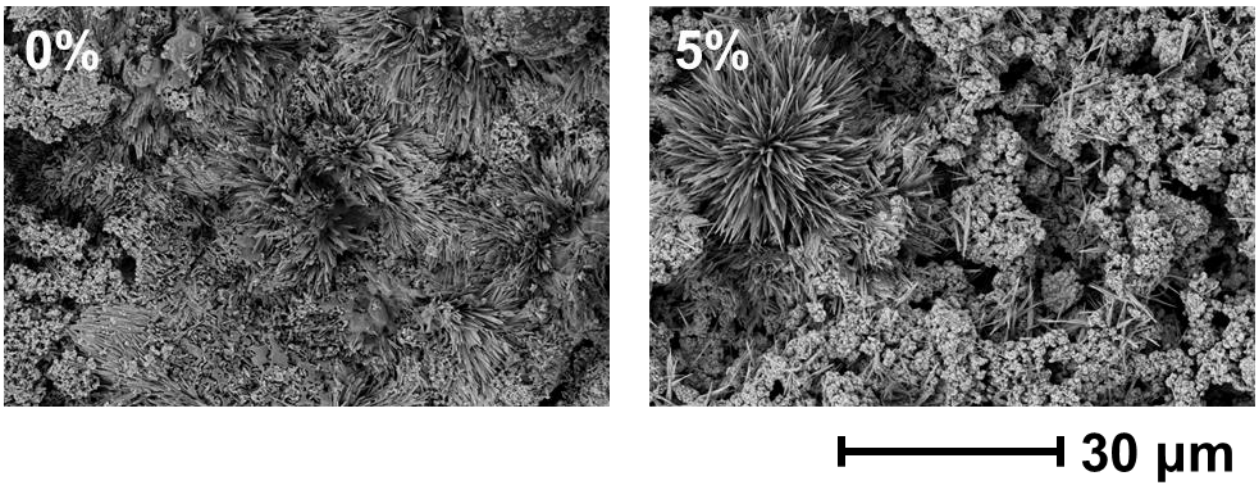

Figure S17. SEM images recorded for the Cu NP GDEs with different CST content (as indicated in the images) after performing CORR electrolysis experiments on them.

Table S2. Faradaic efficiencies during the measurements presented in the manuscript.

Figure 2C								
Sample / electrolyte	**j_{total} / mA cm^{-2}**	**ΣFE / %**	**FE%**					
			H_2	**C_2H_4**	**CH_4**	**n-PrOH**	**EtOH**	**Acetate**
5 wt% CST, 1 M KOH	100	95.41	32.5	34.0	0	11.9	12.3	4.7
	200	94.13	30.0	35.5	0	9.2	12.6	6.8
	300	98.02	31.7	36.3	0	7.7	13.7	8.7
	400	99.50	30.9	34.6	0	7.0	16.5	10.6
	500	99.52	30.9	33.5	0	5.5	17.7	11.9
Figure 2D								
0 wt% CST, 1 M KOH, gas from only gas stream	300	50.10	44.6	1.8	0	0.4	2.5	0.8
0 wt% CST, 1 M KOH, gas from gas+liquid stream	300	89.64	83.3	2.7	0	0.4	2.5	0.8
5 wt% CST, 1 M KOH, gas from only gas stream	300	86.69	20.3	36.3	0	7.7	13.7	8.7
5 wt% CST, 1 M KOH, gas from gas+liquid stream	300	86.23	22.5	33.7	0	7.7	13.7	8.6
10 wt% CST, 1 M KOH, gas from only gas stream	300	86.98	20.3	36.0	0	8.7	15.9	6.0
10 wt% CST, 1 M KOH, gas from gas+liquid stream	300	86.66	21.4	37.9	0	6.9	14.8	4.7

Sample / electrolyte	j_{total} / mA cm^{-2}	ΣFE / %	FE%					
			H_2	C_2H_4	CH_4	n-PrOH	EtOH	Acetate
15 wt% CST, 1 M KOH, gas from only gas stream	300	88.77	24.9	33.6	0	6.5	18.2	5.6
15 wt% CST, 1 M KOH, gas from gas+liquid stream	300	87.76	24.7	36.0	0	5.6	16.7	4.7
20 wt% CST, 1 M KOH, gas from only gas stream	300	37.70	23.4	6.0	0	1.0	5.6	1.7
20 wt% CST, 1 M KOH, gas from gas+liquid stream	300	88.81	70.1	10.4	0	1.0	5.6	1.7
25 wt% CST, 1 M KOH, gas from only gas stream	300	35.13	22.8	5.3	0	0.9	4.1	2.0
25 wt% CST, 1 M KOH, gas from gas+liquid stream	300	95.44	81.5	7.0	0	0.9	4.1	2.0
30 wt% CST, 1 M KOH, gas from only gas stream	300	31.16	19.3	5.3	0	1.0	3.0	2.5
30 wt% CST, 1 M KOH, gas from gas+liquid stream	300	90.50	75.5	8.4	0	1.0	3.0	2.5

Figure 3.								
Sample / electrolyte	**j_{total} / mA cm^{-2}**	**ΣFE / %**	**FE%**					
			H_2	**C_2H_4**	**CH_4**	**n-PrOH**	**EtOH**	**Acetate**
0 wt% CST GDE, 1 M KOH	500	45.26	43.9	0.1	0	0.0	0.7	0.5
5 wt% CST GDE, 1 M KOH	500	99.52	30.9	33.5	0	5.5	17.7	11.9
10 wt% CST GDE, 1 M KOH	500	90.72	29.0	31.5	0	6.9	16.7	6.5
15 wt% CST GDE, 1 M KOH	500	72.98	24.6	22.0	0	3.0	16.8	6.7
20 wt% CST GDE, 1 M KOH	500	26.48	18.6	2.9	0	0.6	2.9	1.6
25 wt% CST GDE, 1 M KOH	500	25.58	18.8	2.8	0	0.6	2.0	1.3
30 wt% CST GDE, 1 M KOH	500	23.19	15.4	3.6	0	0.7	1.8	1.7
5 wt% Nafion GDE, 1 M KOH	500	61.60	38.2	10.9	0	1.7	6.6	4.1
10 wt% Nafion GDE, 1 M KOH	500	36.18	34.0	0.7	0	0.3	0.9	0.3
15 wt% Nafion GDE, 1 M KOH	500	25.32	24.4	0.0	0	0.0	0.8	0.1
20 wt% Nafion GDE, 1 M KOH	500	13.56	13.0	0.0	0	0.0	0.4	0.1
25 wt% Nafion GDE, 1 M KOH	500	3.27	2.8	0.0	0	0.0	0.3	0.1

Sample / electrolyte	j_{total} / mA cm^{-2}	ΣFE / %	FE%					
			H_2	C_2H_4	CH_4	n-PrOH	EtOH	Acetate
30 wt% Nafion GDE, 1 M KOH	500	7.57	7.0	0.0	0	0.0	0.5	0.1
5 wt% PTFE GDE, 1 M KOH	500	55.034	54.7	0.0	0	0.0	0.3	0.0
10 wt% PTFE GDE, 1 M KOH	500	37.05	36.7	0.0	0	0.0	0.3	0.1
15 wt% PTFE GDE, 1 M KOH	500	77.49	77.1	0.0	0	0.0	0.3	0.0
20 wt% PTFE GDE, 1 M KOH	500	3.862	3.5	0.0	0	0.0	0.3	0.1
25 wt% PTFE GDE, 1 M KOH	500	6.80	6.2	0.0	0	0.0	0.5	0.1
30 wt% PTFE GDE, 1 M KOH	500	2.34	1.9	0.0	0	0.0	0.4	0.0
Figure 4B								
5 wt% CST GDE, 1 M LiOH	500	91.58	19.8	41.2	4.4	3.0	19.3	3.8
5 wt% CST GDE, 1 M NaOH	500	91.82	21.0	44.0	0.0	4.7	17.4	4.7
5 wt% CST GDE, 1 M KOH	500	93.37	22.8	37.6	0.0	7.8	20.3	4.9
5 wt% CST GDE, 1 M CsOH	500	91.06	19.0	37.0	0.0	12.6	16.4	6.1

Figure 4C								
Sample / electrolyte	**j_{total} / mA cm^{-2}**	**ΣFE / %**	**FE%**					
			H_2	**C_2H_4**	**CH_4**	**n-PrOH**	**EtOH**	**Acetate**
5 wt% CST GDE, 5 M KOH	200	82.05	10.9	29.5	0.0	9.2	13.9	18.5
	200	86.75	13.7	32.8	0.0	10.2	11.7	18.3
	200	86.19	16.2	32.6	0.0	9.9	9.4	18.1
	200	92.51	19.1	33.6	0.0	11.6	10.0	18.2
	200	94.57	21.5	32.4	0.0	12.0	10.3	18.4
	200	92.79	24.1	31.7	0.0	9.2	8.3	19.5
	200	94.51	26.0	32.1	0.0	10.9	6.9	18.5
	200	93.93	26.5	32.1	0.0	11.3	5.3	18.8
	200	98.08	31.0	32.0	0.0	10.9	5.3	18.9
	200	96.42	33.4	32.4	0.0	9.5	4.2	17.0

Table S2. Faradaic efficiencies during the measurements presented in the Supporting Information.

Figure S5-6								
Sample / electrolyte	**j_{total} / mA cm^{-2}**	**ΣFE / %**	**FE%**					
			H_2	**C_2H_4**	**CH_4**	**n-PrOH**	**EtOH**	**Acetate**
0 wt% CST GDE, 1 M KOH	100	90.0	61.7	14.8	0.0	3.5	9.1	0.9
	200	80.6	67.7	6.1	0.0	0.9	4.9	1.1
	300	50.1	44.6	1.8	0.0	0.4	2.5	0.8
	400	28.7	22.5	0.1	4.6	0.1	0.9	0.5
	500	56.3	43.9	0.1	11.0	0.0	0.7	0.5
5 wt% CST GDE, 1 M KOH	100	95.4	32.5	34.0	0.0	11.9	12.3	4.7
	200	94.1	30.0	35.5	0.0	9.2	12.6	6.8
	300	98.0	31.7	36.3	0.0	7.7	13.7	8.7
	400	99.5	30.9	34.6	0.0	7.0	16.5	10.6
	500	99.5	30.9	33.5	0.0	5.5	17.7	11.9
10 wt% CST GDE, 1 M KOH	100	89.6	32.1	31.7	0.0	11.0	11.5	3.3
	200	93.0	30.3	33.9	0.0	9.0	14.4	5.4
	300	92.1	30.2	32.4	0.0	8.7	14.8	6.0
	400	96.4	29.9	34.3	0.0	8.1	17.7	6.4
	500	90.7	29.0	31.5	0.0	6.9	16.7	6.5
15 wt% CST GDE, 1 M KOH	100	85.6	31.1	31.2	0.0	6.1	13.4	3.8
	200	92.3	29.8	33.7	0.0	8.4	15.4	4.9
	300	92.9	29.0	33.6	0.0	6.5	18.2	5.6
	400	84.8	26.9	29.2	0.0	4.2	18.4	6.1
	500	73.0	24.6	22.0	0.0	3.0	16.8	6.7

Sample / electrolyte	j_{total} / mA cm^{-2}	ΣFE / %	FE%					
			H_2	C_2H_4	CH_4	n-PrOH	EtOH	Acetate
20 wt% CST GDE, 1 M KOH	100	74.0	31.5	21.8	0.0	5.9	13.3	1.5
	200	50.5	26.8	10.7	0.0	2.0	9.3	1.7
	300	37.7	23.4	6.0	0.0	1.0	5.6	1.7
	400	30.9	20.4	4.0	0.0	0.8	4.1	1.6
	500	26.5	18.6	2.9	0.0	0.6	2.9	1.6
25 wt% CST GDE, 1 M KOH	100	64.7	32.6	17.2	0.0	3.8	9.9	1.2
	200	47.1	25.3	9.1	0.0	1.4	8.9	2.4
	300	35.1	22.8	5.3	0.0	0.9	4.1	2.0
	400	29.7	20.3	3.9	0.0	0.8	2.9	1.7
	500	25.6	18.8	2.8	0.0	0.6	2.0	1.3
30 wt% CST GDE, 1 M KOH	100	51.6	28.4	13.5	0.0	2.5	5.9	1.3
	200	40.2	23.9	8.1	0.0	1.6	4.3	2.3
	300	31.2	19.3	5.3	0.0	1.0	3.0	2.5
	400	26.7	16.9	4.5	0.0	0.8	2.3	2.1
	500	23.2	15.4	3.6	0.0	0.7	1.8	1.7

Figure S9								
Sample / electrolyte	**j_{total} / mA cm^{-2}**	**ΣFE / %**	**FE%**					
			H_2	**C_2H_4**	**CH_4**	**n-PrOH**	**EtOH**	**Acetate**
5 wt% Nafion GDE, 1 M KOH	100	90.5	34.6	29.7	0.0	9.7	14.1	2.5
	200	83.0	38.8	25.0	0.0	4.7	11.3	3.2
	300	74.7	38.6	18.1	0.0	3.2	10.4	4.3
	400	67.2	37.9	13.3	0.0	2.3	8.9	4.8
	500	61.6	38.2	10.9	0.0	1.7	6.6	4.1
10 wt% Nafion GDE, 1 M KOH	100	90.3	25.3	33.9	0.0	13.6	12.5	5.0
	200	87.0	29.2	29.2	0.0	8.0	15.4	5.1
	300	84.5	28.1	27.8	0.0	5.5	16.1	7.0
	400	77.2	26.4	22.8	0.0	4.4	15.6	7.9
	500	36.2	34.0	0.7	0.0	0.3	0.9	0.3
15 wt% Nafion GDE, 1 M KOH	100	93.5	24.9	36.0	0.0	13.6	15.4	3.6
	200	86.4	27.2	30.2	0.0	7.0	18.2	3.8
	300	79.8	27.1	24.9	0.0	4.1	18.6	5.2
	400	31.1	26.1	1.4	0.0	0.6	2.4	0.7
	500	25.4	24.4	0.1	0.0	0.0	0.8	0.1
20 wt% Nafion GDE, 1 M KOH	100	83.0	32.4	25.8	0.0	8.0	15.1	1.6
	200	73.2	32.8	19.6	0.0	3.8	13.5	3.4
	300	57.5	30.0	12.5	0.0	2.2	9.5	3.3
	400	36.3	24.4	5.6	0.0	1.1	3.8	1.3
	500	13.6	13.0	0.1	0.0	0.0	0.4	0.1

Sample / electrolyte	j_{total} / mA cm^{-2}	ΣFE / %	FE%					
			H_2	C_2H_4	CH_4	n-PrOH	EtOH	Acetate
25 wt% Nafion GDE, 1 M KOH	100	72.6	32.0	19.7	0.0	7.0	12.3	1.6
	200	63.0	26.3	17.5	0.0	3.8	11.8	3.5
	300	3.5	2.6	0.1	0.0	0.0	0.7	0.2
	400	4.7	4.1	0.1	0.0	0.0	0.4	0.1
	500	3.3	2.8	0.1	0.0	0.0	0.3	0.1
30 wt% Nafion GDE, 1 M KOH	100	67.6	27.8	18.8	0.0	8.0	11.3	1.7
	200	63.0	21.6	18.4	0.0	4.0	14.6	4.4
	300	22.4	16.6	2.0	0.0	0.8	2.4	0.6
	400	9.1	8.1	0.1	0.0	0.0	0.7	0.2
	500	7.6	7.0	0.1	0.0	0.0	0.5	0.1

Figure S11								
Sample / electrolyte	**j_{total} / mA cm^{-2}**	**ΣFE / %**	**FE%**					
			H_2	**C_2H_4**	**CH_4**	**n-PrOH**	**EtOH**	**Acetate**
5 wt% Nafion GDE, 1 M KOH, gas from only gas stream	100	46.56	27.8	18.8	0	n.a.	n.a.	n.a.
	200	39.99	21.6	18.4	0	n.a.	n.a.	n.a.
	300	18.56	16.6	2.0	0	n.a.	n.a.	n.a.
	400	8.22	8.1	0.1	0	n.a.	n.a.	n.a.
	500	7.08	7.0	0.1	0	n.a.	n.a.	n.a.
5 wt% Nafion GDE, 1 M KOH, gas from gas+liquid stream	100	55.90	35.6	20.3	0	n.a.	n.a.	n.a.
	200	65.66	48.5	17.2	0	n.a.	n.a.	n.a.
	300	88.41	87.5	0.9	0	n.a.	n.a.	n.a.
	400	97.69	97.5	0.2	0	n.a.	n.a.	n.a.
	500	99.94	99.9	0.1	0	n.a.	n.a.	n.a.
Figure S12								
5 wt% PTFE GDE, 1 M KOH	100	53.087	40.9	4.6	0.0	2.1	4.7	0.8
	200	66.27	64.4	0.0	0.0	0.0	1.2	0.7
	300	73.69	73.0	0.0	0.0	0.0	0.6	0.2
	400	67.95	67.5	0.0	0.0	0.0	0.4	0.0
	500	55.035	54.7	0.0	0.0	0.0	0.3	0.0
10 wt% PTFE GDE, 1 M KOH	100	37.63	32.1	0.0	0.0	1.4	3.8	0.4
	200	73.30	71.7	0.0	0.0	0.2	1.0	0.4
	300	69.71	68.9	0.0	0.0	0.0	0.6	0.2
	400	43.73	43.3	0.0	0.0	0.0	0.4	0.0
	500	37.05	36.7	0.0	0.0	0.0	0.3	0.1

Sample / electrolyte	j_{total} / mA cm^{-2}	ΣFE / %	FE%					
			H_2	C_2H_4	CH_4	n-PrOH	EtOH	Acetate
15 wt% PTFE GDE, 1 M KOH	100	35.67	26.7	2.1	0.0	1.7	4.5	0.5
	200	86.01	82.9	0.0	0.0	0.0	1.6	1.5
	300	88.14	86.7	0.0	0.0	0.0	0.9	0.5
	400	80.82	79.9	0.0	0.0	0.0	0.6	0.3
	500	77.50	77.1	0.0	0.0	0.0	0.3	0.0
20 wt% PTFE GDE, 1 M KOH	100	50.05	46.4	0.0	0.0	0.7	2.6	0.4
	200	78.16	76.6	0.0	0.0	0.0	1.0	0.5
	300	46.20	45.6	0.0	0.0	0.0	0.5	0.1
	400	28.32	27.9	0.0	0.0	0.0	0.4	0.0
	500	3.86	3.5	0.0	0.0	0.0	0.3	0.1
25 wt% PTFE GDE, 1 M KOH	100	22.85	17.3	0.0	0.0	1.0	4.2	0.4
	200	18.05	15.0	0.0	0.0	0.3	2.3	0.5
	300	13.09	11.3	0.0	0.0	0.0	1.4	0.5
	400	11.46	10.4	0.0	0.0	0.0	0.8	0.3
	500	6.80	6.2	0.0	0.0	0.0	0.5	0.1
30 wt% PTFE GDE, 1 M KOH	100	45.15	29.0	3.1	0.0	3.1	9.0	0.9
	200	31.66	25.5	1.0	0.0	0.3	3.6	1.2
	300	27.21	23.9	0.0	0.0	0.3	2.1	0.8
	400	10.06	9.3	0.0	0.0	0.0	0.6	0.1
	500	2.34	1.9	0.0	0.0	0.0	0.4	0.0